Journal of Global Positioning Systems (2025)
Vol. 21, Issue 2: 109-123
DOI:10.5081/jgps.21.2.109

Integrity Assessment and Error Modeling of BDS PPP-B2b Signal-in-Space for ARAIM

Yaping Huang, Yun Wu*, Yaxuan Li, Lang Feng
School of Geodesy and Geomatics, Wuhan University, Wuhan 430079, China
* Correspondence: ywu@sgg.whu.edu.cn

Abstract： BDS provides PPP (Precise Point Positioning) service via the B2b signal transmitted by BDS-3 GEO satellites for users in China and surrounding areas. For high-precision safety-of-life applications, the integrity of its Signal-in-Space (SIS) is critical. In addition, Advanced Receiver Autonomous Integrity Monitoring (ARAIM), as a key approach of GNSS integrity monitoring, relies on reliable prior integrity parameters of SIS to ensure its results trustworthy. Aiming at integrity assessment and SIS error modeling of PPP-B2b, this study first computes the PPP-B2b Signal-in-Space Errors (SISEs) from January 1, 2021, to December 31, 2024, by applying PPP-B2b correction messages to the BDS-3 CNAV1 broadcast ephemerides and comparing the corrected orbits and clocks with precise ephemerides. Based on the four-year SISEs datasets, the integrity assessments show that PPP-B2b SISEs exhibit improved smoothness compared to CNAV1. The RMS of Orbit-Only User Range Errors (UREs) improves by 5.7%, while clock performance shows only marginal improvement for four satellites. There is no significant spatial correlation of SISEs between satellites. Furthermore, the empirical distribution of Instantaneous UREs (IUREs) indicates that most satellites exhibit non-zero mean, multimodality, and asymmetry characteristics which contradict the ARAIM assumption of zero-mean Gaussian distribution. Additionally, the User Range Accuracy (URA) values broadcast by PPP-B2b are overly tight and fail to adequately bound the actual IUREs, which improperly describe the deviations of UREs. To obtain reliable SISEs stochastic model for PPP-B2b ARAIM users, the integrity support parameters under SIS nominal condition are derived by taking use of the Two-Step Gaussian overbounding method. The derived SIS integrity parameters can be referred by ARAIM users and the integrity assessment provides a key reference for subsequent optimization of system integrity performance.

Keywords: BDS-3; PPP-B2b service; Signal-in-Space User Range Errors; Integrity

1. Introduction

The Precise Point Positioning (PPP) service of the BeiDou Navigation Satellite System (BDS) was officially launched on July 31, 2020. This service broadcasts high-precision orbit and clock correction parameters of the BDS-3 system, via the B2b signal channel of BDS-3 GEO satellites, primarily targeting PPP users in China and surrounding regions. The accuracy of the PPP-B2b Signal-in-Space (SIS) is crucial for ensuring the decimeter-level real-time wide-area service provided by BDS-3, and the signal integrity plays a vital role in meeting the high-reliability requirements of intelligent applications such as autonomous driving.

The accuracy of SIS is typically evaluated by comparing broadcast ephemerides with

post-processed precise ephemerides to directly quantify orbit and clock, or indirectly through positioning performance. Based on these methods, several studies have investigated the accuracy of PPP-B2b signals. Jiang et al. (2023) analyzed the satellite orbit errors using five days of PPP-B2b correction messages, and reported the RMS of orbit better than 0.13m (radial), 0.32m (along-track), and 0.29m (cross-track), respectively. Huang and Meng (2021) used four days of PPP-B2b correction message and estimated the RMS of clock offset to be 4.48ns, but the STD was better than 0.10ns. Meng et al. (2024) compared the positioning accuracy of PPP-B2b with Japan's QZSS CLAS service using seven days of data, and found that under a single GPS constellation, PPP-B2b exhibited slightly lower performance. Cai et al. (2023) validated the user positioning accuracy using 15 days of correction messages, achieving horizontal accuracy better than 0.06m(east), 0.05m(north), and 0.13m(up) through PPP processing. However, these studies were all based on short-term datasets spanning only a few weeks, and are insufficient to comprehensively reflect the long-term stability and reliability of the PPP-B2b service.

In terms of SIS integrity research, the User Range Error (URE) is commonly adopted as a metric to quantify actual SIS performance. The User Range Accuracy (URA) broadcast in the navigation message represents a conservative estimate of the standard deviation of UREs, and reflects the system's prior performance commitment. As defined in the GPS SPS Performance Standards (DoD, 2008), potential SIS faults are identified using a threshold of 4.42×URA. Signals exceeding this limit are flagged as suspected faults; otherwise, they are treated as fault-free SIS (SIS in nominal condition). Previous studies have analyzed the integrity of BDS-2 Navigation Message, showing that the 2-meter broadcast URA of BDS-2 cannot overbound the SIS UREs of all satellites (Wang et al., 2018). In another study, the Two-Step Gaussian overbounding method was applied to model the fault-free SIS performance of BDS-3 (Wang et al., 2024). Walter and Blanch (2015) developed error bounding models for fault-free SIS signals of GPS and GLONASS, providing overbounding parameters for all satellites. Nevertheless, to date, there is no publicly available study that systematically evaluates the integrity performance of the BDS-3 PPP-B2b service signal.

Due to the short time span of corrections and the lack of integrity-focused analyses in existing research on PPP-B2b signals, this study presents a comprehensive evaluation of the accuracy and integrity of BDS PPP-B2b signals using long-term data from January 1, 2021 to December 31, 2024. We first introduce the data sources and availability of the broadcast ephemerides, precise ephemerides, and PPP-B2b correction messages used in the analysis. After excluding suspected faulty SIS samples, we analyze the empirical distribution of IUREs for each satellite and evaluate the overbounding capability of the broadcast URA against actual errors. Finally, we apply the Two-Step Gaussian overbounding method to construct a PPP-B2b SIS error model suitable for Advanced Receiver Autonomous Integrity Monitoring (ARAIM) applications.

2. Data sources and availability

2.1. Data sources

As defined in the GPS Standard Positioning Service Performance Standard (DoD, 2008), the Signal-in-Space Errors (SISEs) refer to the UREs caused by broadcast orbit and clock offsets in GNSS navigation messages. In this study, satellite orbit and clocks from BDS-3 CNAV1 navigation messages are corrected using PPP-B2b correction messages. The corrected orbit and clocks are then compared with post-processed precise ephemerides provided by the International GNSS Service (IGS) analysis centers, and the difference is taken as the PPP-B2b SISEs. Therefore, the datasets required for this study include BDS-3 CNAV1 broadcast ephemerides, PPP-B2b correction messages, and precise ephemerides.

The BDS-3 CNAV1 broadcast ephemerides can be downloaded from the official FTP server of the China Satellite Navigation Office Test and Assessment Research Center (ftp://pub:tarc@

ftp2.csno-tarc.cn/cnav). CNAV1 provides 18 Keplerian orbital parameters for all BDS-3 satellites at each full hour, which are used to compute satellite positions and clocks at any epoch within the message validity period (CSNO, 2019). Currently, precise orbit and clock products for BDS-3 are publicly available from several IGS analysis centers, including the Center for Orbit Determination in Europe (CODE), the German Research Centre for Geosciences (GFZ), and Wuhan University (WHU). Based on the availability and accuracy assessment of products from these institutions (Ma et al., 2024), this study uses WHU precise ephemerides (15-minute sampling interval) for data prior to March 17, 2021, and switches to CODE products (5-minute interval) thereafter.

The PPP-B2b correction messages used in this study were received in real time by a FinaGeo receiver located in Wuhan, Hubei Province, China, covering the time period from January 1, 2021, to December 31, 2024. Due to receiver maintenance and other interruptions, the data is incomplete in certain periods, resulting in a total of 1,116 days of valid PPP-B2b navigation message data.

2.2. Data Availability

PPP-B2b SISEs can only be derived for a given satellite and epoch when CNAV1 broadcast ephemerides, PPP-B2b correction messages, and precise ephemerides are all available and deemed healthy. In this study, the empirical correction rate is defined as the ratio of the number of epochs for which valid PPP-B2b corrections can be applied to the total number of natural epochs. Considering that PPP-B2b provides a regional service primarily for China and neighboring areas, we analyze the data availability with reference to the regional visibility and coverage of MEO and IGSO satellites for ground users.

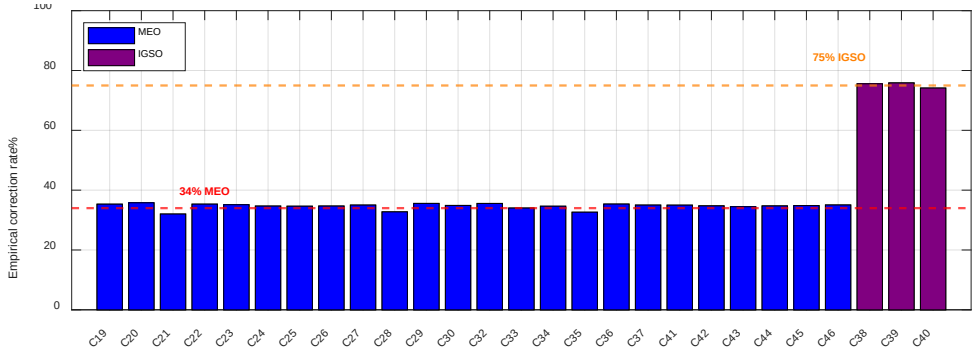

Fig. 1 Empirical correction rate of PPP-B2b correction messages

For example, satellite C19 had approximately 302,300 natural epochs during the study period, among which around 106,770 epochs had available PPP-B2b SISEs, resulting in an empirical correction rate of 35.3%. The overall availability of PPP-B2b SISEs for all BDS-3 satellites is illustrated in Fig. 1. The red dashed line represents the theoretical ground visibility rate of MEO satellites (DoD US, 2008), while the orange dashed line corresponds to that of IGSO satellites (Wen et al., 2007). The results show that the average availability of PPP-B2b SISEs is 35.7% for MEO satellites and 75.2% for IGSO satellites, which is close to the expected reference values, indicating that the PPP-B2b correction messages used in this study are reasonably complete and representative.

Further statistical analysis reveals that, in 91.9% of epochs, the number of BDS-3 satellites effectively corrected by PPP-B2b messages ranged from 9 to 13, with a maximum of 16 satellites corrected simultaneously.

3. Computation of PPP-B2b SIS Errors

The overall processing workflow for computing PPP-B2b SISEs is illustrated in Fig. 2. PPP-B2b correction messages are first matched and associated

with the corresponding CNAV1 broadcast ephemerides. The orbit, clock, and Differential Code Bias (DCB) corrections are subsequently applied, after which the precise ephemerides are adjusted for satellite antenna phase center variations. The corrected satellite positions are compared against the PPP-B2b corrected orbits in the Earth-Centered, Earth-Fixed (ECEF) coordinate frame to compute orbit difference vectors. These difference vectors are then decomposed into the satellite-based coordinate frame consisting of the radial (R), along-track (A), and cross-track (C) directions. For clock offset processing, the common bias between precise and broadcast clock products is removed to obtain the residual clock offsets. These clock offsets are combined with the orbit errors to compute three types of UREs. Finally, a fault detection threshold is defined to filter out epochs with abnormal signal errors. The orbit errors, clock offsets, and corresponding UREs values of the fault-free epochs are retained for subsequent analysis.

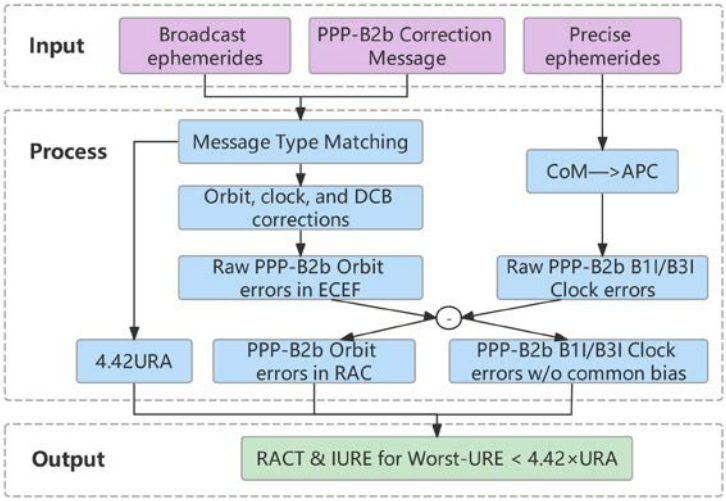

Fig. 2 Procedure for obtaining fault-free SISEs of PPP-B2b

3.1. Message Type Matching

To manage and associate different types of correction messages within the PPP-B2b service, BDS-3 adopts four types of versioning parameters. The detailed association rules are illustrated in Fig. 3.

Fig. 3 The association rules of PPP-B2b correction messages

The Issue of Data Number for Navigation (IODN) in the PPP-B2b orbit correction messages must be consistent with the Issue of Data Clock (IODC) in the CNAV1 broadcast ephemerides. Since the IODC in broadcast ephemerides changes immediately upon ephemeris updates, while the IODN in PPP-B2b corrections is subject to a transmission delay, it is necessary to continue using the previous ephemeris

during the initial period of update. This ensures that the IODN matches the IODC, thereby maintaining the validity of the correction information (CSNO 2020).

For the association of orbit and clock correction parameters, PPP-B2b correction messages use the IOD Corr as the version control identifier. Orbit corrections are updated every 48 seconds, while clock corrections are updated every 6 seconds. In most cases, both types of corrections share the same IOD Corr and remain in a valid matching state. However, if the clock corrections are updated independently, leading to a change in IOD Corr, a temporary mismatch may occur. In such cases, users should revert to using the clock correction value from the previous epoch that matches the orbit correction, until the next orbit correction update restores the version consistency (Xu et al., 2021).

3.2. CNAV1 corrected by PPP-B2b Correction Messages

3.2.1. Corrected Orbit

The orbit correction vectors provided by PPP-B2b are expressed in the satellite's orbital coordinate system, while the satellite positions computed from the CNAV1 broadcast ephemerides are given in the ECEF coordinate frame. Therefore, coordinate transformation is required prior to applying the corrections. The transformation is performed using the following equations:

$$\mathrm{e}_{\mathrm{R}} = \frac{\mathrm{X}_{\mathrm{brdc}}}{\left|\dot{\mathrm{X}}_{\mathrm{brdc}}\right|} \tag{1}$$

$$\mathrm{e}_{\mathrm{C}} = \frac{\mathrm{X}_{\mathrm{brdc}} \times \dot{\mathrm{X}}_{\mathrm{brdc}}}{\left|\mathrm{X}_{\mathrm{brdc}} \times \dot{\mathrm{X}}_{\mathrm{brdc}}\right|} \tag{2}$$

$$\mathrm{e}_{\mathrm{A}} = \mathrm{e}_{\mathrm{C}} \times \mathrm{e}_{\mathrm{R}} \tag{3}$$

$$\mathrm{X}_{\mathrm{orbit}} = \mathrm{X}_{\mathrm{brdc}} - \left[\mathrm{e}_{\mathrm{R}} \quad \mathrm{e}_{\mathrm{A}} \quad \mathrm{e}_{\mathrm{C}}\right] \cdot \delta O \tag{4}$$

Here, $\mathrm{e}_{\mathrm{R}}, \mathrm{e}_{\mathrm{A}}, \mathrm{e}_{\mathrm{C}}$ represent the radial, along-track, and cross-track unit vectors, respectively; $\mathrm{X}_{\mathrm{brdc}}$ and $\dot{\mathrm{X}}_{\mathrm{brdc}}$ denote the satellite's position and velocity vectors from the broadcast ephemeris; $\delta O = \left[\delta R \quad \delta A \quad \delta C\right]^T$ are the PPP-B2b orbit correction components; $\mathrm{X}_{\mathrm{orbit}}$ is the corrected satellite position vector.

3.2.2. Corrected Clock

The clock derived directly from CNAV1 clock parameters is based on the B3I frequency. The PPP-B2b clock correction can be directly applied to it. At epoch k, the correction formula for satellite i is as follows:

$$t^i_{PPP_{\mathrm{B3I}}}(k) = t^i_{CNAN1}(k) - \frac{\delta t^i(k)}{c} \tag{5}$$

where $t^i_{CNAV1}(k)$ is the clock offset from broadcast ephemeris, $\delta t^i(k)$ is the PPP-B2b clock correction, and $t^i_{PPP_{\mathrm{B3I}}}(k)$ is the corrected satellite clock. c is the speed of light.

To enable comparison between the corrected result and the precise clock from the precise ephemeris, it is necessary to apply DCB correction to $t^i_{PPP_{\mathrm{B3I}}}(k)$, aligning it with the B1I/B3I frequency combination used by the precise clock. The correction formula is as follows:

$$t^i_{PPP}(k) = t^i_{PPP_{\mathrm{B3I}}}(k) + \frac{f^2_{B1I}}{f^2_{B1I} - f^2_{B3I}} \cdot DCB^i(k) \tag{6}$$

Here, DCB_i is the DCB between B3I and B1I signals; $f_{\mathrm{B1I}}, f_{\mathrm{B3I}}$ are the respective signal frequencies; $t^i_{PPP}(k)$ is the clock value corrected to match the frequency reference of the precise ephemeris.

There still exists a time system bias between PPP-B2b and precise ephemerides after DCB correction (Wu et al., 2017). This bias is absorbed by receiver clock parameters during positioning (Dai et al., 2021) but must be removed when computing SISEs. A more robust approach is adopted in this study, where the median clock offset $\bar{t}^i_{PPP}(k)$ at epoch k is used as the system bias. The satellite clock offset with the system bias removed is given by:

$$\hat{t}^i_{PPP}(k) = t_{i,PPP}(k) - \bar{t}_{i,PPP}(k) \tag{7}$$

Finally, the PPP-B2b clock offset is obtained by directly subtracting the precise clock from $t^i_{PPP}(k)$. The calculation formula is as follows:

$$\Delta T^i(k) = \hat{t}^i_{PPP}(k) - t^i_{sp3}(k) \tag{8}$$

Where $\Delta T^i(k)$ denotes the PPP-B2b clock offset of satellite i at epoch ~~t~~ k, and $t^i_{sp3}(k)$ represents the precise clock of satellite i at the same epoch.

3.3. Computation of URA

In the PPP-B2b correction messages, two

parameters (URA class and URA value) are broadcast to compute the URA, and both are represented as 3-bit binary numbers in the message. When both parameters are 000, the URA is marked as unknown, indicating that the corresponding orbit and clock corrections are unreliable. When both parameters are 111, the URA exceeds 5466.5 mm, meaning the satellite no longer meets high-precision accuracy requirements. The URA is computed as (CSNO 2020):

$$URA[mm] \le 3^{URA_{class}}(1+0.25\times URA_{value})-1 \quad (9)$$

3.4. Computation of URE

URE quantifies the projection of orbit and clock offsets onto the line-of-sight direction between the satellite and the user. It can be classified into: IURE (Instantaneous URE), Worst-URE and Orbit-Only URE.

For IUREs computation, the Asia-Pacific region is gridded at 5° latitude/longitude intervals. For a user at position u, the IUREs of satellite i are calculated as (Zheng and Pan, 2022):

$$IURE_{i,u}(k)=\frac{[R_i(k)\ \ A_i(k)\ \ C_i(k)]}{\sqrt{1+d^2-2d\sin(\theta_u)}}\begin{bmatrix} d-\sin(\theta_u) \\ -\cos(\theta_u)\cos(\varphi_u) \\ -\cos(\theta_u)\sin\varphi_u \end{bmatrix}-c\cdot T_i(k) \quad (10)$$

where d denotes the ratio of the satellite-to-Earth-center distance to the Earth's radius. The "latitude θ_u" and "longitude φ_u" refer to parameters defined in the satellite orbital coordinate system, rather than the geographic latitude and longitude of the user's position. $R^i(k), A^i(k), C^i(k)$ represent radial, along-track, and cross-track orbit errors of satellite i at epoch k, respectively.

The calculation of Worst-UREs can be performed via the analytical method (Wang et al., 2018) or the grid method. However, since the analytical method yields the absolute value of URE, it is unsuitable for the subsequent correlation analysis of SISEs. Therefore, we adopt the maximum absolute IUREs across all visible users of satellite i at epoch k as the Worst-URE. The calculation formula is as follows:

$$Worst-URE_i(t)=IURE^i_{u^*}(t),\quad \text{where } u^*=\arg\max_u\left|IURE^i_u(t)\right| \quad (11)$$

Here, $Worst-URE^i(t)$ represents the Worst-URE of satellite i at epoch t, u^* denotes the user with the worst IURE, and $IURE^i_u(t)$ is the URE of the satellite i projected onto user u at epoch t.

The Orbit-Only UREs isolates orbit-induced ranging error and are computed as:

$$orbit\_only\ URE^i(k)=\sqrt{w_1^2R^i(k)^2+w_2^2(A^i(k)^2+C^i(k)^2)} \quad (12)$$

For BDS-3 satellites, under a 0° elevation mask, typical Earth radius ratios are: $w_1=0.981$, $w_2=0.136$ for MEO satellites and $w_1=0.992$, $w_2=0.089$ for IGSO satellites (Montenbruck et al., 2018).

3.5. Exclusion of SIS faults

Section 5.1 shows that PPP-B2b URA values tightly overbound IUREs but fail to reliably characterize actual SISE performance. If a 4.42 × URA threshold were used, many signals would be falsely flagged as faults. To robustly identify fault-free signals, the following filtering steps are adopted:

(1) Initial Filtering: Exclude signals with Worst-UREs > 5 m → yields fault-free SIS$^{(1)}$.

(2) RMS Thresholding: Compute RMS of Worst-UREs in fault-free SIS$^{(1)}$, denoted as rms$^{(1)}$; exclude signals with Worst-UREs > 4.42×rms$^{(1)}$ → yields fault-free SIS$^{(2)}$.

(3) Iterative Refinement: Repeat the above step until no further signals in fault-free SIS$^{(j+1)}$ exceed 4.42×rms$^{(j)}$.

(4) Final Dataset: The resulting fault-free SIS$^{(j+1)}$ set is regarded as the fault-free dataset.

Applying this filtering strategy to data from Jan 1, 2021 to Dec 31, 2024, approximately 0.32% of data points with Worst-UREs exceeding 4.42×0.9903 m

were identified as suspected faults and excluded. The resulting fault-free datasets contains on average 103,997 epochs per MEO satellite and 218,966 epochs per IGSO satellite, providing a robust basis for subsequent analysis.

4. Comparisons of PPP-B2b and CNAV1

4.1. SISEs Time series: PPP-B2b vs CNAV1

To directly observe the differences between PPP-B2b SISEs and CNAV1 SISEs, this study selected six satellites (C20, C21, C35, C37, C40, and C46) and analyzed their radial orbit error time series (Fig. 4) and clock offset time series (Fig. 5) over the period from March 11 to March 16, 2022.

It should be noted that PPP-B2b provides high-precision correction services primarily for users in China and its surrounding regions. Consequently, when a satellite is outside the service coverage area, no PPP-B2b correction message is available, leading to temporal discontinuities in Fig. 4 and Fig. 5.

The results show that, compared to CNAV1, PPP-B2b exhibits significantly better smoothness in both orbit errors and clock offsets series. This is mainly because CNAV1 ephemerides are updated at hourly intervals, and extrapolation errors accumulate over time, resulting in discontinuities at the beginning of each hour. In contrast, PPP-B2b provides orbit and clock updates at much higher rates which can effectively mitigate extrapolation errors and reduce the fluctuations in the error sequences.

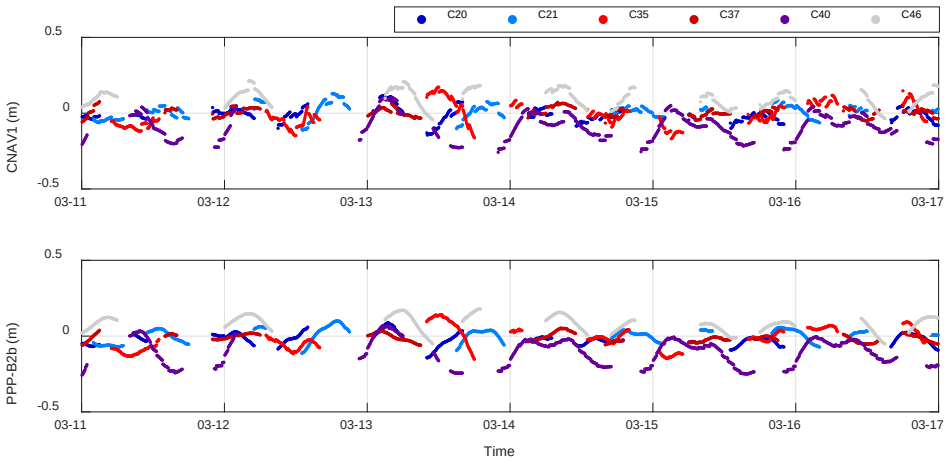

Fig. 4: Errors series of radial orbit (CNAV1 and PPP-B2b, March 7–12, 2021)

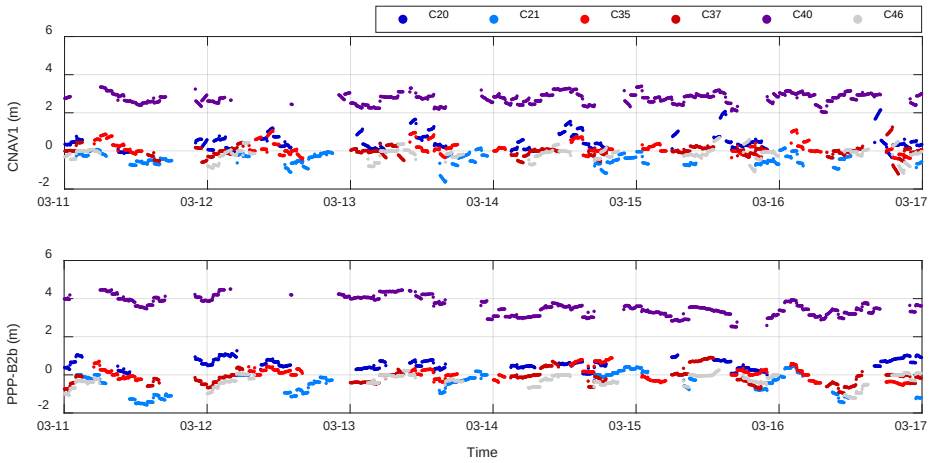

Fig. 5: Errors series of clock offset (CNAV1 and PPP-B2b, March 7–12, 2021)

4.2. RMS Comparison

Fig. 6 presents a comparison of the Orbit-Only UREs for each satellite before and after applying PPP-B2b corrections, using the RMS as the accuracy metric. The results show that the Orbit-Only UREs for both CNAV1 broadcast ephemerides and PPP-B2b corrected data remain within 0.2m. Specifically, the MEO satellites exhibit Orbit-Only UREs around 0.1m, while IGSO satellites (C38, C39, and C40) show slightly higher errors of approximately 0.15m, indicating that IGSO satellites have slightly lower orbit accuracy compared to MEO satellites.

Compared to the orbit errors derived from CNAV1 alone, the PPP-B2b corrections yield an improvement in Orbit-Only UREs accuracy by 5.4% for MEO satellites and 6.0% for IGSO satellites. After correction, the RMS values improve to 9.80 cm for MEO and 15.77 cm for IGSO satellites, respectively.

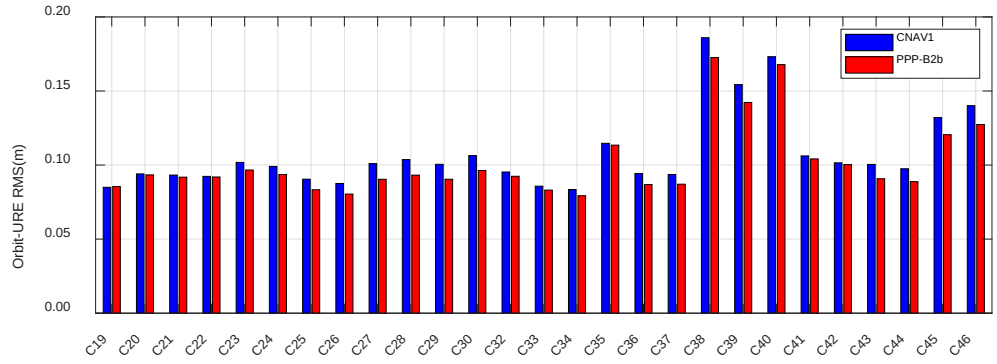

Fig. 6: RMS of Orbit-Only UREs for CNAV1 and PPP-B2b (2021–2024)

Fig. 7 illustrates the changes in the RMS of satellite clock offsets before and after applying PPP-B2b corrections. As shown in the figure, the clock offsets accuracy of all other satellites deteriorates except for four satellites (C19, C20, C30, and C36). This degradation is attributed to the presence of noticeable biases in the satellite clock corrections provided by PPP-B2b, a finding that is consistent with the results reported by Zhong et al. (2023). These biases vary across satellites. Although in PPP processing such clock biases can be absorbed into the ambiguity term of the phase observation equations, the corresponding deviations in pseudorange observations are not canceled out and will propagate into the positioning domain, thereby causing positioning errors. Therefore, in the context of SIS integrity analysis, these biases should not be subtracted from the satellite clock offsets.

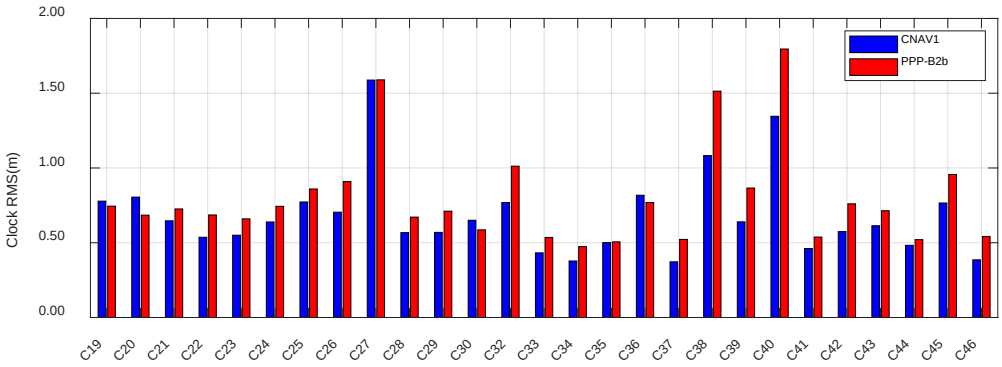

Fig. 7 RMS of clock offset errors from CNAV1 and PPP-B2b (2021–2024)

5. Integrity Analysis of PPP-B2b Signal-in-Space

5.1. Distribution of SISE

The reliability of ARAIM monitoring depends on the accuracy of the SISE integrity model. This model assumes that the IUREs follow a normal distribution N(0,URA), and that IUREs from different satellites are statistically independent. Therefore, this study analyzes both the distribution and spatial correlation of IUREs.

The IUREs for each satellite were computed using Equation (10), and a normalized histogram were plotted with a bin width of 0.1 m. The vertical axis of the histogram represents the relative frequency of IUREs values within each bin, with the sum of all bar heights equal to unity. As shown in Fig. 8, the normalized histograms of satellites C23, C26, and C29 exhibit non-zero means and characteristics resembling a normal distribution. The 12 satellites presented in Fig. 9 have means close to zero; however, their distribution kurtosis shows sharp peaks, flat tops, and asymmetry, indicating non-ideal distribution characteristics. Another set of 12 satellites shown in Fig. 10 exhibits non-normal features such as skewed peaks and heavy tails (C36). Given these distribution characteristics differ from the assumptions of the ARAIM integrity model, further overbounding analysis of the IURE is required to establish a more accurate and reliable integrity model.

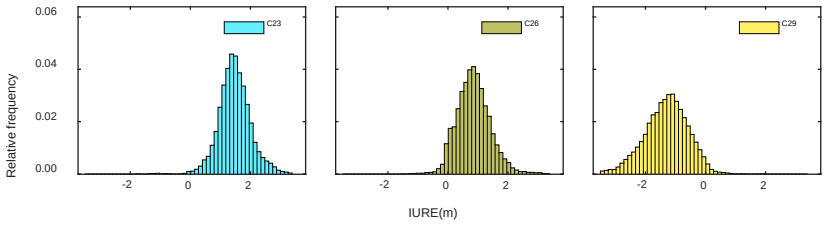

Fig. 8 Normalized histograms of IUREs with non-zero means

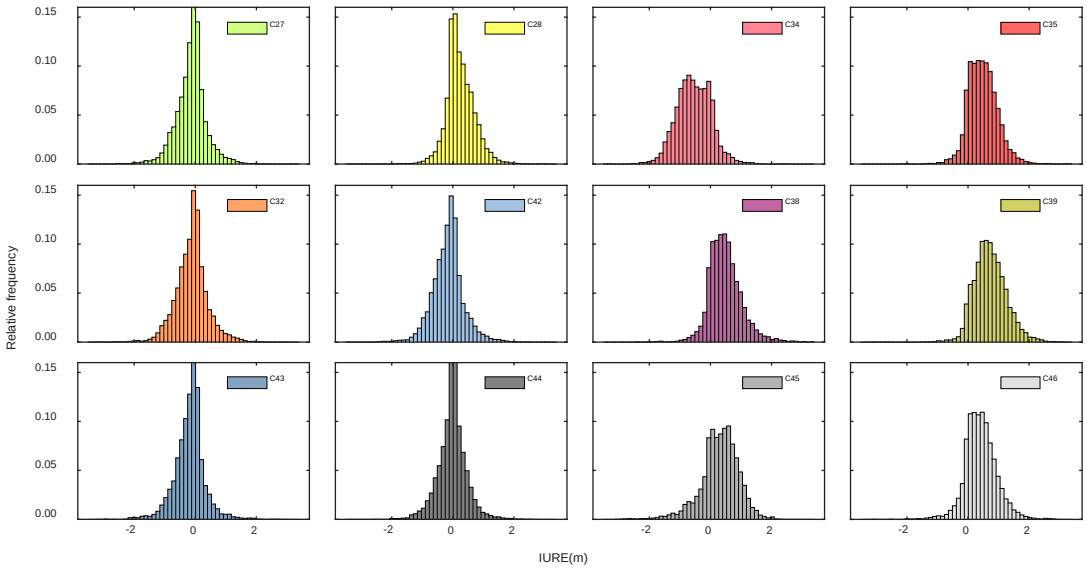

Fig. 9 Normalized histograms of IURE with kurtosis deviations from normality

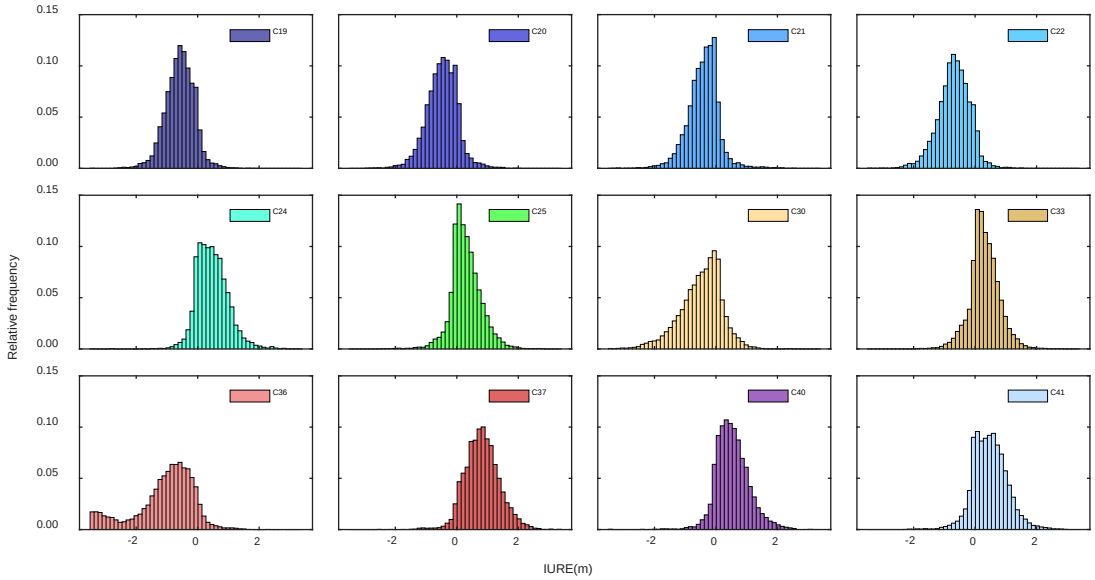

Fig. 10 Normalized histograms of IURE with skewness deviations from normality

5.2. Correlation of SISEs

Fig. 11 presents the spatial correlation coefficients of Worst-UREs among MEO and IGSO satellites. The analysis reveals that approximately 79.2% of satellite pairs exhibit weak correlation, with coefficients falling within the range of (-0.2, 0.2). However, some satellite pairs demonstrate significant correlation. For instance, the correlation coefficient between C29 and C43 reaches 0.89.Whether such correlated SISEs could lead to protection level underbounding the position error requires further investigation in future studies (FAA, 2023).

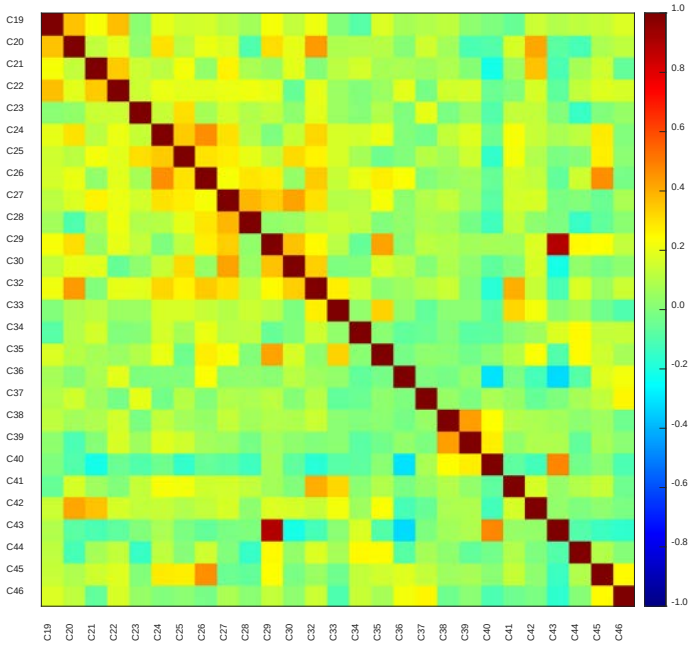

Fig. 11: Correlation of Worst-UREs Among Satellites

5.3. URA overbounding of IUREs

The URA reflects a priori precision of satellite SIS and is a key indicator for evaluating the performance of satellite navigation services. To further analyze the actual URA broadcast behavior in the PPP-B2b service, we conducted a statistical analysis of the URA values from all satellites over the

four-year period from 2021 to 2024. The results are shown in Fig. 12.

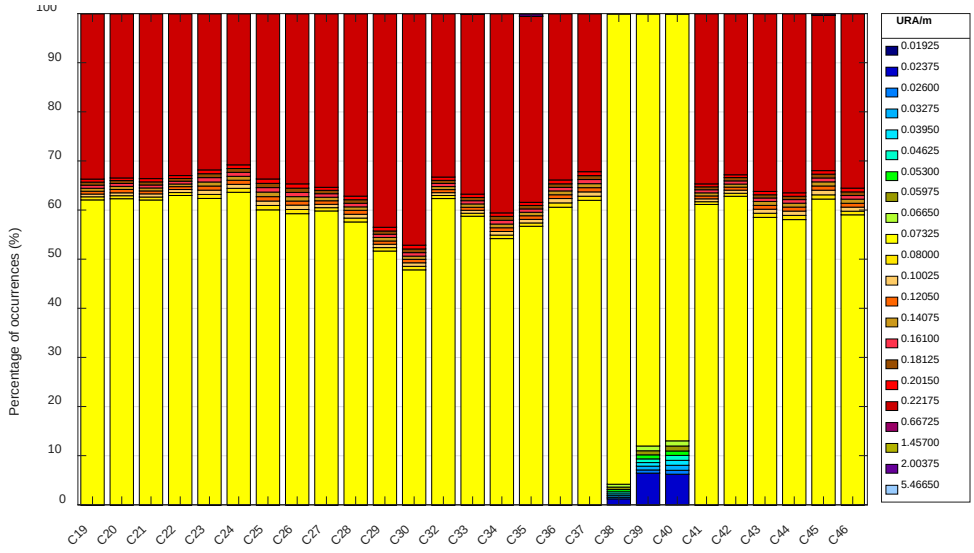

Fig. 12 URA of PPP-B2b correction message

The URA values in PPP-B2b have a resolution of 0.25mm, with a value range from 0.25 mm to 5466.5mm. Compared with the URA in CNAV1 broadcast ephemerides, PPP-B2b offers a wider range and finer resolution. As shown in Fig. 12, the minimum and maximum broadcast URA values in PPP-B2b are 0.01925m and 5.4665m, respectively. In the figure, yellow bars represent URA values of 0.07325m, while red bars represent values of 0.22175m. Among them, MEO satellites broadcast the 0.07325m URA value for 59.5% of the time and the 0.22175m value for 35.4% of the time. IGSO satellites tend to have smaller URA values, with 90.23% of URA values being 0.22175m.

To verify whether these URA values can correctly overbound the IUREs, we normalize IUREs based on the assumption that IUREs follow a normal distribution with standard deviation URA, as shown in the following equation:

$$x^i(k) = \frac{IURE^i(k)}{URA^i(k)} \quad (13)$$

Where $IURE^i(k)$ and $URA^i(k)$ are the IUREs and broadcast URA of satellite i at epoch k, respectively. If the published URA values can properly describe IUREs, the normalized values $x^i(k)$ should satisfy $P\left(\left|x^i(t)\right|<1\right)\approx 68\%$ and $P\left(x^i(t)<2\right)\approx 95\%$.

Fig. 13 shows the Cumulative Distribution Function (CDF) of the normalized IUREs. The blue dashed line indicates 68% confidence, and the red dashed line indicates 95% confidence. The results show that all satellite IUREs are overly overbounded by the published URA, meaning the PPP-B2b URA is overly optimistic. If ARAIM users build stochastic models using these URA values to compute protection level, it may lead to hazardous misleading information.

5.4. Gaussian Overbounding of IUREs

The above analysis indicates that PPP-B2b SISEs do not follow a normal distribution, and the broadcast URA values do not adequately characterize the accuracy of IUREs over time. Therefore, ARAIM users need to reestablish a reliable integrity model for SISEs.

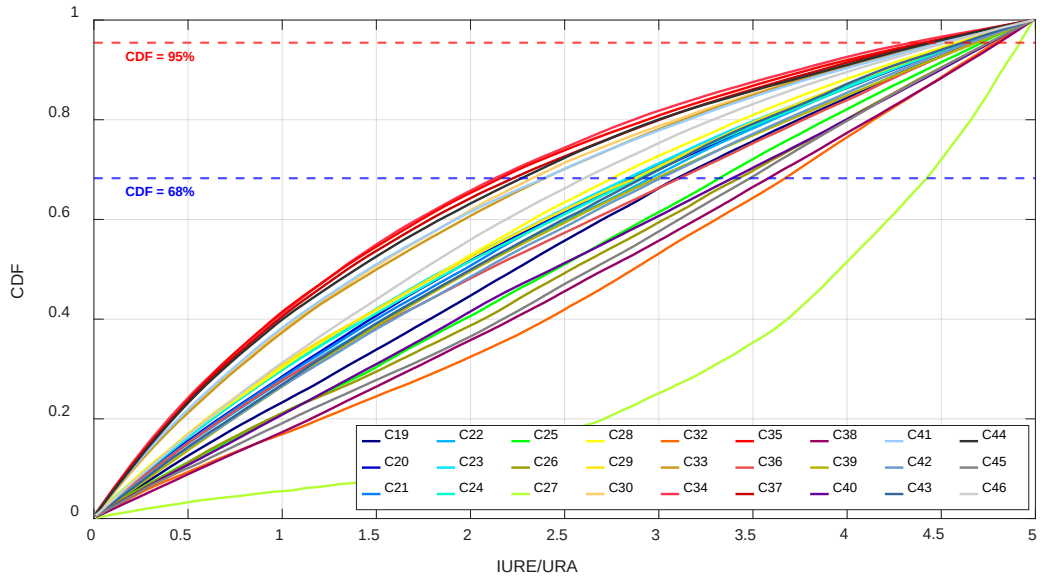

Fig. 13 CDF of IUREs after PPP-B2b Correction

The original method for bounding such errors was defined by RTCA (DeCleene, 2000) to construct conservative probabilistic boundaries. However, methods such as symmetric unimodal CDF Overbounding only apply to symmetric, unimodal distributions, and the Paired Gaussian Overbounding method requires the bounding CDF to cover the empirical CDF across the entire range, which is overly restrictive (Rife et al., 2006). To address these limitations, Blanch proposed the "Two-Step" Gaussian Overbounding method (Blanch et al., 2019), which combines the strengths of the previous approaches. This method allows Gaussian bounding of errors without strict distributional assumptions or full CDF containment. The "Two-Step" method proceeds as follows:

(1) Construct a symmetric unimodal intermediate distribution

The error samples are first divided into fixed-width intervals. A symmetric unimodal intermediate distribution is constructed that overbounds the empirical distribution in the CDF sense. This is done by enforcing increasing frequency counts up to the median bin, then mirroring to form the right-hand side. The result is a smoothed, piecewise uniform distribution with symmetric structure. Although this intermediate distribution does not preserve the original mean or skewness of the sample data, it facilitates a better Gaussian fit in the next step.

(2) Apply Gaussian Overbounding to the intermediate distribution

A Gaussian distribution is then fitted such that it fully overbounds one side (left or right) of the intermediate distribution's CDF. This avoids the over-conservativeness of full-range CDF bounding. The left and right overbounds are constructed independently, and the more conservative of the two is selected as the integrity bound for ARAIM.

We applied the "Two-Step" method to determine the IUREs overbounding parameters $N(b,\sigma_{URA})$ for each satellite in the PPP-B2b system. The results are shown in Fig. 14. It can be seen from the figure that, except for satellites C33 and C34, most BDS-3 satellites exhibit deviations of 0.3–1m in their overbounding models, with the b values of the two IGSO satellites C38 and C40 exceeding 1.5m. As for the parameter σ_{URA}, all satellites are approximately 1m. Combining the Gaussian Overbounding results with the PPP-B2b broadcast URA information shown in Fig. 12, it can be observed that the σ_{URA} of IGSO satellites is not generally smaller than that of MEO satellites, contrary to the prior expectation.

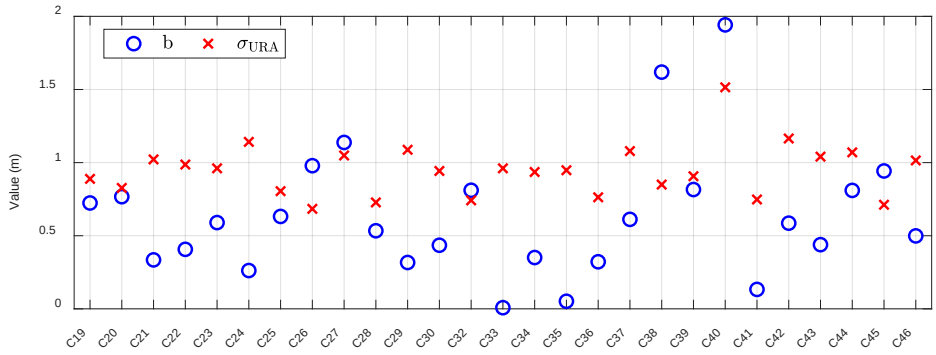

Fig. 14 Two-Step Gaussian overbounding parameters b and σ_{URA}

6. Conclusion

Based on long-term PPP-B2b correction messages from January 1, 2021 to December 31, 2024, we systematically evaluated the integrity of the PPP-B2b SIS under normal operating conditions, and obtained integrity support parameters suitable for PPP-B2b ARAIM users. The main conclusions are as follows:

(1) Compared to CNAV1, the PPP-B2b corrections exhibit better smoothness in the orbit and clock error sequences. Regarding orbit accuracy, PPP-B2b corrections improve the Orbit-Only UREs of MEO and IGSO satellites by 5.4% and 6.0%, respectively, with the post-correction RMS being 9.80cm and 15.77cm. However, in terms of clock accuracy, most satellites experienced varying degrees of degradation after PPP-B2b correction, with only four satellites showing slight improvements in clock precision.

(2) Analysis of the empirical distribution of PPP-B2b SIS IUREs revealed that most satellites exhibit characteristics such as asymmetry, multimodality, and heavy tails. Further correlation analysis of Worst-UREs indicates that most satellites have weak inter-satellite correlations, except for a significant correlation between C29 and C43, with a coefficient as high as 0.89. Overall, PPP-B2b SISEs do not satisfy the ARAIM assumption that "SISEs follows independent zero-mean Gaussian distributions."

(3) Statistics of PPP-B2b broadcast URA values show that the URA is generally underestimated. Specifically, 99.959% of MEO satellite URA values less than 0.22175m, while 99.998% of IGSO satellite URA values less than 0.07325m. Further comparative analysis indicates that the PPP-B2b broadcast URA does not effectively characterize the actual IUREs distribution, posing a risk of overly tight overbounding and thus cannot serve as reliable integrity prior information.

(4) We employed the "Two-Step" Gaussian Overbounding method to establish a PPP-B2b Signal-in-Space Errors model. The results show that the overbounding parameters b for most BDS-3 satellites range from 0.3m to 1m, with corresponding σ_{URA} values of approximately 1m. These modeling results can provide prior integrity information for the application of PPP-B2b in ARAIM.

7. References

Jiang, W., Chen, X., et al (2023): Accuracy evaluation on satellite orbit determination of BDS-3 PPP-B2b service. GNSS World of China, 48(1), 32–36, doi: 10.12265/j.gnss.2022154.

Huang, L. and Meng, X. (2021): Accuracy analysis of precise point positioning using BDS-3 PPP-B2b signals. Journal of Geodesy and Geodynamics, 41(5), 516–519, doi: 10.14075/j.jgg.2021.05.014.

Meng, X., Liu, C., et al (2024**):** Comparative analysis of performance of BDS-3 precise point positioning service and QZSS centimeter-level augmentation service for experiment. Journal of

Geomatics Science and Technology, 40(6), 593–600, doi: 10.3969/j.issn.1673-6338.2024.06.005

Cai, Z., Fang, R., et al (2023**):** Accuracy evaluation of BDS-3 B2b signal correction broadcast ephemeris and PPP application. GNSS World of China, 48(1), 64–70, doi: 10.12265/j.gnss.2022217.

DOD US (2008**):** Global positioning system standard positioning service performance standard (4th ed.), U.S. Department of Defense.

Wang, Z., Shao, W., et al (2018**):** Characteristics of BDS signal-in-space user ranging errors and their effect on advanced receiver autonomous integrity monitoring performance. Sensors, 18(24), 4475, doi: 10.3390/s18124475.

Wang, D., Qin, H., et al. (2024**):** Clock error analysis and compensation for LEO signal of opportunity positioning. IEEE Sensors Journal, 24(8), 12716–12727, doi: 10.1109/JSEN.2024.3370249.

Walter, T., and Blanch, J. (2015**):** Keynote – Characterization of GNSS clock and ephemeris errors to support ARAIM. In Proceedings of the ION 2015 Pacific PNT Meeting (pp. 920–931). Honolulu, HI: Institute of Navigation.

CSNO (2019**):** BeiDou satellite navigation system signal in space interface control document public service signal B1C (Version 1.0) [EB/OL]. Accessed on January 1, 2019.

Ma, R., Ma, L. and Shi, Z. (2024**):** Comparative analysis of BDS precise ephemeris accuracy based on long baseline. Journal of Navigation and Positioning, 12(3), 120–129. doi: 10.16547/j.cnki.10-1096.20240314

Wen, Y., Liu, Q., et al (2007**):** The effect of TT&C deployment on the regional satellite navigation system. Journal of National University of Defense Technology, 29(1), 1–6.

CSNO (2020**):** BeiDou navigation satellite system signal in space interface control document: Precise point positioning service signal PPP-B2b (Version 1.0). China Satellite Navigation Office.

Xu, Y., Yang, Y. and Li, J. (2021**):** Performance evaluation of BDS-3 PPP-B2b precise point positioning service. GPS Solutions, 25, 142, doi: 10.1007/s10291-021-01175-2

Wu, Y., Liu, X. et al (2017**):** Long-term behavior and statistical characterization of BeiDou signal-in-space errors. GPS Solutions, 21, 1907–1922, doi: 10.1007/s10291-017-0663-0.

Dai, P., Xing, J. et al (2021**):** The Effect of BDS-3 Time Group Delay and Differential Code Bias Corrections on Positioning. Applied Sciences, 11(1), 104, doi: 10.3390/app11010104.

Zheng, J. and Pan, S. (2022**):** GNSS signal-in-space integrity assessment and analysis. Journal of Time and Frequency, 45(1), 59–74, doi: 10.13875/j.issn.1674-0637.2022-01-0059-16.

Wang, Z., Shao, W. et al (2018**):** Characteristics of BDS signal-in-space user ranging errors and their effect on advanced receiver autonomous integrity monitoring performance. Sensors, 18(12), 4475, doi: 10.3390/s18124475.

Satellite Navigation Branch (2023**):** Advanced receiver autonomous integrity monitoring performance analysis report (Report No. 12), ANG-E66, FAA William J. Hughes Technical Center, www.nstb.tc.faa.gov

DeCleene, B. (2000**):** Defining pseudorange integrity-Overbounding. In Proceedings of the 13th International Technical Meeting of the Satellite Division of the Institute of Navigation (ION GPS 2000) (pp. 1916–1924). Salt Lake City, UT: The Institute of Navigation.

Rife, J., Pullen, S., Enge, P., & Pervan, B. (2006**):** Paired overbounding for nonideal LAAS and WAAS error distributions. IEEE Transactions on Aerospace and Electronic Systems, 42(4), 1386–1395, doi: 10.1109/TAES.2006.314579.

Blanch, J., Walter, T. and Enge, P. (2019**):** Gaussian bounds of sample distributions for integrity analysis. IEEE Transactions on Aerospace and Electronic Systems, 55(4), 1806–1815, doi: 10.1109/TAES.2018.2876583.

Montenbruck, O., Steigenberger, P. and Hauschild, A. (2018**):** Multi-GNSS signal-in-space range error assessment: Methodology and results. Advances

in Space Research, 61(12), 3020–3038. https://doi.org/10.1016/j.asr.2018.03.041

Zhong, S., Zhang, Z., Chen, G. and Qian, L. (2023**):** Performance evaluation of BDS-3 PPP-B2b signal-in-space. Hydrographic Surveying, 43(1), 49–52, doi: 10.3969/j.issn.1671-3044.2023.01.011

Authors

Yaping Huang is a Master's student in Geodesy and Surveying Engineering at Wuhan University, focusing on GNSS integrity monitoring.

Yun Wu is an associate professor in the School of Geodesy and Geomatics, Wuhan University, China. She obtained her B.Sc., Master and Ph.D. degrees in Geodesy and Surveying Engineering from Wuhan University. Her research interests are in the area of GNSS high accuracy positioning and integrity monitoring.

Yaxuan Li is a Master's candidate at School of Geodesy in Wuhan University. His research focus on GNSS integrity monitoring.

Lang Feng is a Master's student at the School of Geodesy and Geomatics, Wuhan University. His research centers on GNSS PPP-RTK positioning and integrity monitoring.